STUDY ON MECHANISM OF FANGYI QINGFEI DECOCTION AGAINST COVID-19 ASSOCIATED LUNG AND KIDNEY INJURY BASED ON NETWORK PHARMACOLOGY AND MOLECULAR DOCKING

Zhi Zuo[1*], Kai Liao[2*], Huailian Liu[3*], Ran Yu[4], Haiqing Chen[4], Wanpeng Wang[4]
[1]Department of Cardiology, The First Affiliated Hospital of Nanjing Medical University, Nanjing 210000, Jiangsu, China - [2]School of Pharmacy, Shihezi University, Key Laboratory of Xinjiang Phytomedicine Resources and Utilization, Ministry of Education, Shihezi, Xinjiang 832002, China - [3]Department of Hospital Infection-Control Huai'an maternal and child health care hospital, Medical College of Yangzhou University, Huai'an 223400, Jiangsu, China - [4]Department of Central Laboratory, Lianshui People's Hospital, Kangda college of Nanjing Medical University, Huai'an 223400, Jiangsu, China
[*]*contributed equally to this work*

ABSTRACT

Introduction*: The outbreak of Coronavirus Disease 2019 (COVID-19) in Wuhan, China, was caused by severe acute respiratory syndrome coronavirus 2 (SARS-CoV-2). The present study aims to explore the potential antiviral and lung or kidney tissue-protecting mechanisms of Fangyi Qingfei Decoction (FYQFD) on COVID-19 based on network pharmacology and molecular docking method.*

Materials and methods*: Traditional Chinese Medicine Systems Pharmacology (TCMSP) was used to search the compounds and targets of FYQFD, and GeneCards database was used to search the pathological targets of acute lung or kidney injury; The intersection method was used to obtain the targets related to the therapeutic effect of FYQFD. Protein-protein interaction (PPI) network was constructed by Search Tool For Recurring Instances of Neighbouring Genes (STRING) database and the hub target genes were identified by calculating node degree. Molecular docking was performed based on the hub compounds and hub target genes and the SARS-CoV-2 3CL hydrolase (SARS-CoV-2 3CLpro) and angiotensin converting enzyme II (ACE2), respectively.*

Results*: Total 159 potential active components, corresponding to 203 targets associated lung and kidney injury, were screened from FYQFD. GO function enrichment analysis revealed 123 biological process (BP) items ($P < 0.05$), 75 signal pathways ($P < 0.05$) were screened out after KEGG pathway enrichment analysis. Furthermore, molecular docking indicated that main active compounds kaempferol, quercetin, wogonin, luteolin and acacetin in FYQFD exhibited higher affinity among AKT1, ALB, IL6, TP53, VEGFA, TNF, JUN, CASP3, EGFR, MAPK1 with SARS-CoV-2 3CLpro and ACE2.*

Conclusion*: By this procedure, the present study enhanced the understanding of the potential therapeutic mechanism of FYQFD, that the partial compounds in FYQFD can bind with SARS-CoV-2 3CLpro and ACE2, and acting on many targets to regulate multiple signaling pathways, thus exerting the therapeutic effect on COVID-19.*

Keywords: *COVID-19, quercetin,kaempferol, network pharmacology, molecular docking.*

DOI: 10.19193/0393-6384_2021_4_307

Received *October 15, 2020;* ***Accepted*** *March 20, 2021*

Introduction

Novel coronavirus pneumonia is an infectious disease induced by severe acute respiratory syndrome coronavirus 2 (SARS-CoV-2), which was officially named coronavirus disease 2019 (COVID-19) by the WHO on February 11, 2020[(1)]. The COVID-19 has spread in more than 210 countries around the world, bringing serious disasters to human survival and social development, and has a wide and far-reaching impact on the international political and economic structure[(2)]. According to the data released by World

Health Organization (WHO), the COVID-19 was diagnosed in 110,384,747 cases at 2:51pm CET on February 20, 2021, and 2,446,008 cases died. It is of great importance to search for rapid and effective therapeutic drugs for COVID-19, so that can prevent the disease from spreading and reduce the damage.

However, there is currently no specific drug or vaccine for COVID-19 and while the pandemic is progressing rapidly. Except for the typical symptoms of pneumonia and acute respiratory distress syndrome (ARDS), the COVID-19 may progress to or even died of acute kidney injury (AKI), shock, and multiple organ failure (MOF)[3]. Since the virus receptor angiotensin-converting enzyme 2 (ACE2) is highly expressed in the kidney, kidney is also a sensitive target for sars-cov-2. Increasing evidence showed that COVID-19 may cause kidney damage, as indicated by the occurrence of proteinuria, hematuria and elevated serum creatinine (Scr) on admission, with the high incidence of AKI[4]. The typical renal pathologic abnormalities including acute tubular necrosis, endothelial damage and capillary occlusions, deposition of complement complex on tubules, tubulointerstitial lymphocyte infiltration was identified in autopsy reports[5,6]. Kidney injury may result from hemodynamic factors, dysfunctional immune responses[7], or direct viral infection of kidney cells which had been proved that there are SARS-CoV-2 mRNA and protein in renal tissue[8]. Therefore, the current treatment of critical patients not only focuses on improving the symptoms of the respiratory system, but also on actively protecting the renal function and improving the prognosis.

Traditional Chinese medicine (TCM), a form of complementary and alternative medicine, is one of the oldest medical systems in the world, and has accumulated a lot of experience in prevention and treatment of epidemic disease in the past. According to the theoretical foundation of plague, it is convinced that Chinese medicine is an effective treatment for COVID-19[9]. "Fangyi Qingfei Decoction (FYQFD)" is a combination of Yu Ping Feng powder, Sen Mai powder, Shen Zhu powder and Gui Zhi decoction, with a clinic modifications and supplements, which are made by doctors of TCM department and pharmacists in Lianshui County People's Hospital, and it has been approved by Huai'an natural science research plan (NO. HAB202011) for the prevention of front-line medical staff, and no obvious side effects such as fever and rash were found in the clinical research process. Embrased 14 herbs, the prescription are all legal traditional Chinese medicine included in Pharmacopoeia of the People's Republic of China (2015 Edition), including Huang Qi (Hedysarum Multijugum Maxim), Bai Zhu (Atractylodes), Fang Feng (Saposhnikoviae Radix), Gui Zhi (Cinnamomi Ramulus), Bai Shao (Paeoniae Radix Alba), Gan Jiang (Zingiberis Rhizoma), Da Zao (Jujubae Fructus), Bei Sha Shen (Glehniae Radix), Mai Dong (Ophiopogon Japonicus), Tai Zi Shen (Pseudostellariae Radix), Wu Wei Zi (Schisandrae Chinensis Fructus), Cang Zhu (Atractylodes Lancea), Jie Geng (Platycodon Grandiforus) and Xing Ren (Amygdalus Communis Vas). The prescription pays attention to both exorcism and strengthening the body, with the key point of "Evil has a way out, healthy qi can recover" based on basic theory of TCM. The main therapeutic characteristics of TCM are multi-component, multi-target and multi-channel. Network pharmacology is a new research strategy that integrates systems biology, multidirectional pharmacology, computational biology and molecular simulation docking technology, which coincides with the holistic view and system theory of TCM. This technology is capable of revealing the mechanism of synergistic action of multi-molecular drugs on human body by constructing drug-component-target network. In this study, we screened out the active components of FYQFD and predicted the possible targets of each active components in the prevention and treatment of COVID-19 associated lung and kidney injury. Then the molecular docking technology was used to explore the feasibility of FYQFD in the treatment of lung and kidney injury induced by COVID-19.

Materials and methods

Collection of ingredients of FYQFD and screening

The components of herbs used in FYQFD were collected from the Traditional Chinese Medicine Systems Pharmacology (TCMSP) database (http://tcmspw.com/tcmsp .php)[10] and related references, with the keyword “Huang Qi”, “Bai Zhu”, “Fang Feng”, “Gui Zhi”, “Bai Shao”, “Gan Jiang”, “Da Zao”, “Bei Sha Shen”, “Mai Dong”, “Tai Zi Shen”, “Wu Wei Zi”, “Cang Zhu”, “Jie Geng” and “Xing Ren”. The candidates of effective components from the TCMSP were retained based on the standard that their oral bioavailability (OB) ≥ 30% and if their drug likeness (DL) ≥ 0.18[11]. To obtain targets of each identified compound, putative targets were also predicted from the TCMSP database. Afterward, the

official gene symbol of obtained target proteins were standardized in the UniProt (https://www.uniprot.org), with the properties set to "human".

Prediction of targets associated with lung or kidney injury

Genes related to lung or kidney injury were retrieved from the Human Gene Database (GeneCards, https://www.genecards.org/)[12], the species was selected as "Homo sapiens" with the keyword "kidney injury", "renal injury", "lung injury" or "pulmonary injury". The targets were also sent to the UniProt Database for normalization. Renal or lung injury associated targets were mapped to those of FYQFD using Venn plotting online software (http://bioinformatics.psb.ugent.be/webtools/Venn/) to obtain potential targets of FYQFD against COVID-19 associated lung and kidney injury.

Enrichment analyses

GO (Gene Ontology) function and pathway enrichment analyses of hub genes were performed based on DAVID (Database for Annotation, Visualization and Integrated Discovery) (http://david.abcc.ncifcrf.gov/). FDR < 0.05 was considered to be of significantly statistic difference.

Network construction and analysis

To clarify the interaction between potential targets of FYQFD against COVID-19 associated lung and kidney injury, we uploaded the list of overlapping proteins to the Search Tool for the Retrieval of Interacting Genes/Proteins database (STRING) (https://string-db.org/) for protein-protein interaction (PPI) analysis, with the species limited to "Homo sapiens" and the confidence score cut-off set at 0.4, and the rest of the settings were default. The Cytoscape (v.3.5.1) software was used to visualize and analyse the interaction network. The cytoHubba plug-in of the Cytoscape software was used to identify the top-10 genes as hub genes by means of caculated degree.

Molecular docking

The hub genes with more connected active component in herbs were linked by molecular docking. The structural formula (PDB format) of SARS-CoV-2 3CLpro, ACE2 and the hub genes were downloaded from RCSB Protein Data Bank (PDB, http://www.rcsb.org/). The structural formula (mol2 format) of active component in herbs were downloaded from the TCMSP; the structural formula (SDF format) of remdesivir, which used as a control in present study, was downloaded from PubChem database (https://pubchem.ncbi.nlm.nih.gov/) and converted to PDB format with OpenBabel-3.0 software. The targets were processed by removing water, adding hydrogen, optimising amino acids and selecting the magnetic field, and the pdbqt format was saved as a pair acceptor. Atomic charges and assigned atom types were added to compounds in the PDB format, and the pdbqt format was saved as a docked ligand. The active site for molecular docking was determined and size was set. Finally, Autodock Vina v.1.1.2 was run to perform molecular docking[13]. PyMOL v.2.3 software was used to visualize the docking results, and based on the binding conformations of the docking results of each compound, the docking results with lower binding energy and better conformation were selected.

Results

Active components screening for FYQFD

It is well accepted that Chinese herbal plants contain many bioactive compounds, and the therapeutic effects of herbal treatments are achieved via compound/target interaction. In this study, we started our work by researching the active ingredients contained in FYQFD and their protein targets. As a result, components of 14 herbal medicines in FYQFD were collected (Table 1), of which Huang Qi, Bai Zhu, Fang Feng, Gui Zhi, Bai Shao, Gan Jiang, Da Zao, Bei Sha Shen, Tai Zi Shen, Wu Wei Zi, Cang Zhu, Jie Geng and Xing Ren were identified from the TCMSP database; Mai Dong (also kwown as Mai Men Dong) were obtained by literature mining[14]. Next, according to the screening criteria of the ADME, including the OB and DL, 128 active ingredients of FYQFD were retrieved after removing the duplicated targets.

Chinese names	Latin names	Dosage(g)	No. of total ingredients	No. of ingredients passing ADME filtration
Huang Qi	Hedysarum Multijugum Maxim	15	87	20
Bai Zhu	Atractylodes Macrocephala Koidz.	10	55	7
Fang Feng	Saposhnikoviae Radix	10	173	18
Gui Zhi	Cinnamomi Ramulus	10	220	7
Bai Shao	Paeoniae Radix Alba	10	85	13
Gan Jiang	Zingiberis Rhizoma	10	148	5
Da Zao	Jujubae Fructus	10	133	29
Bei Sha Shen	Glehniae Radix	10	35	8
Tai Zi Shen	Pseudostellariae Radix	10	25	8
Wu Wei Zi	Schisandrae Chinensis Fructus	5	130	8
Cang Zhu	Atractylodes Lancea	6	49	9
Jie Geng	Platycodon Grandiforus	10	102	7
Xing Ren	Amygdalus Communis Vas	6	113	19
Mai Dong	Ophiopogon Japonicus	10	-	1

Table 1: The constitution of Fangyi Qingfei Decoction (FYQFD).

Details of all bioactive ingredient information are provided in the Supplementary Table S1.

Mol ID	Molecule Name	MW	OB (%)	DL
Huang Qi (Hedysarum Multijugum Maxim)				
MOL000211	Mairin	456.78	55.38	0.78
MOL000239	Jaranol	314.31	50.83	0.29
MOL000296	hederagenin	414.79	36.91	0.75
MOL000033	(3S,8S,9S,10R,13R,14S,17R)-10,13-dimethyl-17-[(2R,5S)-5-propan-2-yloctan-2-yl]-2,3,4,7,8,9,11,12,14,15,16,17-dodecahydro-1H-cyclopenta[a]phenanthren-3-ol	428.82	36.23	0.78
MOL000354	isorhamnetin	316.28	49.6	0.31
MOL000371	3,9-di-O-methylnissolin	314.36	53.74	0.48
MOL000374	5'-hydroxyiso-muronulatol-2',5'-di-O-glucoside	642.67	41.72	0.69
MOL000378	7-O-methylisomucronulatol	316.38	74.69	0.3
MOL000379	9,10-dimethoxypterocarpan-3-O-β-D-glucoside	462.49	36.74	0.92
MOL000380	(6aR,11aR)-9,10-dimethoxy-6a,11a-dihydro-6H-benzofurano[3,2-c]chromen-3-ol	300.33	64.26	0.42
MOL000387	Bifendate	418.38	31.1	0.67
MOL000392	formononetin	268.28	69.67	0.21
MOL000398	isoflavanone	316.33	109.99	0.3
MOL000417	Calycosin	284.28	47.75	0.24
MOL000422	kaempferol	286.25	41.88	0.24
MOL000433	FA	441.45	68.96	0.71
MOL000438	(3R)-3-(2-hydroxy-3,4-dimethoxyphenyl)chroman-7-ol	302.35	67.67	0.26
MOL000439	isomucronulatol-7,2'-di-O-glucosiole	626.67	49.28	0.62
MOL000442	1,7-Dihydroxy-3,9-dimethoxy pterocarpene	314.31	39.05	0.48
MOL000098	quercetin	302.25	46.43	0.28
Bai Zhu (Atractylodes Macrocephala Koidz)				
MOL000020	12-senecioyl-2E,8E,10E-atractylentriol	312.39	62.4	0.22
MOL000021	14-acetyl-12-senecioyl-2E,8E,10E-atractylentriol	355.44	60.31	0.31
MOL000022	14-acetyl-12-senecioyl-2E,8Z,10E-atractylentriol	356.45	63.37	0.3
MOL000028	α-Amyrin	426.8	39.51	0.76
MOL000033	(3S,8S,9S,10R,13R,14S,17R)-10,13-dimethyl-17-[(2R,5S)-5-propan-2-yloctan-2-yl]-2,3,4,7,8,9,11,12,14,15,16,17-dodecahydro-1H-cyclopenta[a]phenanthren-3-ol	428.82	36.23	0.78
MOL000049	3β-acetoxyatractylone	274.39	54.07	0.22
MOL000072	8β-ethoxy atractylenolide III	276.41	35.95	0.21
Fang Feng (Saposhnikoviae Radix)				
MOL000011	(2R,3R)-3-(4-hydroxy-3-methoxy-phenyl)-5-methoxy-2-methylol-2,3-dihydropyrano[5,6-h][1,4]benzodioxin-9-one	386.38	68.83	0.66
MOL011730	11-hydroxy-sec-o-beta-d-glucosylhamaudol_qt	292.31	50.24	0.27
MOL011732	anomalin	426.5	59.65	0.66
MOL011737	divaricatacid	320.32	87	0.32
MOL011740	divaricatol	334.35	31.65	0.38
MOL001941	Ammidin	270.3	34.55	0.22
MOL011747	ledebouriellol	374.42	32.05	0.51
MOL011749	phellioptorin	300.33	43.39	0.28
MOL011753	5-O-Methylvisamminol	290.34	37.99	0.25
MOL002644	Phellopterin	300.33	40.19	0.28
MOL000359	sitosterol	414.79	36.91	0.75
MOL000173	wogonin	284.28	30.68	0.23
MOL000358	beta-sitosterol	414.79	36.91	0.75
MOL001494	Mandenol	308.56	42	0.19
MOL001942	isoimperatorin	270.3	45.46	0.23
MOL003588	Prangenidin	270.3	36.31	0.22
MOL007514	methyl icosa-11,14-dienoate	322.59	39.67	0.23
MOL013077	Decursin	328.39	39.27	0.38
Gui Zhi (Cinnamomi Ramulus)				
MOL001736	(-)-taxifolin	304.27	60.51	0.27
MOL000358	beta-sitosterol	414.79	36.91	0.75
MOL000359	sitosterol	414.79	36.91	0.75
MOL000492	(+)-catechin	290.29	54.83	0.24
MOL000073	ent-Epicatechin	290.29	48.96	0.24
MOL004576	taxifolin	304.27	57.84	0.27
MOL011169	Peroxyergosterol	428.72	44.39	0.82
Bai Shao (Paeoniae Radix Alba)				
MOL001930	benzoyl paeoniflorin	584.62	31.27	0.75
MOL000359	sitosterol	414.79	36.91	0.75
MOL000358	beta-sitosterol	414.79	36.91	0.75
MOL000422	kaempferol	286.25	41.88	0.24
MOL001919	(3S,5R,8R,9R,10S,14S)-3,17-dihydroxy-4,4,8,10,14-pentamethyl-2,3,5,6,7,9-hexahydro-1H-cyclopenta[a]phenanthrene-15,16-dione	358.52	43.56	0.53
MOL001921	Lactiflorin	462.49	49.12	0.8
MOL001924	paeoniflorin	480.51	53.87	0.79
MOL000492	(+)-catechin	290.29	54.83	0.24
MOL000211	Mairin	456.78	55.38	0.78
MOL001910	11alpha,12alpha-epoxy-3beta-23-dihydroxy-30-norolean-20-en-28,12beta-olide	470.71	64.77	0.38
MOL001928	albiflorin_qt	318.35	66.64	0.33
MOL001925	paeoniflorin_qt	318.35	68.18	0.4
MOL001918	paeoniflorgenone	318.35	87.59	0.37
Gan Jiang (Zingiberis Rhizoma)				
MOL002464	1-Monolinolein	354.59	37.18	0.3
MOL002501	[(1S)-3-[(E)-but-2-enyl]-2-methyl-4-oxo-1-cyclopent-2-enyl] (1R,3R)-3-[(E)-3-methoxy-2-methyl-3-oxoprop-1-enyl]-2,2-dimethylcyclopropane-1-carboxylate	360.49	62.52	0.31
MOL002514	Sexangularetin	316.28	62.86	0.3
MOL000358	beta-sitosterol	414.79	36.91	0.75
MOL000359	sitosterol	414.79	36.91	0.75
Da Zao (Jujubae Fructus)				
MOL012921	stepharine	297.38	31.55	0.33
MOL012940	Spiradine A	311.46	113.52	0.61
MOL012946	zizyphus saponin I_qt	472.78	32.69	0.62
MOL012961	jujuboside A_qt	472.78	36.67	0.62
MOL012976	coumestrol	268.23	32.49	0.34
MOL012980	Daechuine S6	548.75	46.48	0.79
MOL012981	Daechuine S7	514.74	44.82	0.83
MOL012986	Jujubasaponin V_qt	472.78	36.99	0.63
MOL012989	Jujuboside C_qt	472.78	40.26	0.62
MOL012992	Mauritine D	342.46	89.13	0.45
MOL001454	berberine	336.39	36.86	0.78
MOL001522	(S)-Coclaurine	285.37	42.35	0.24
MOL000211	Mairin	456.78	55.38	0.78
MOL000449	Stigmasterol	412.77	43.83	0.76
MOL003410	Ziziphin_qt	472.78	66.95	0.62
MOL000358	beta-sitosterol	414.79	36.91	0.75
MOL004350	Ruvoside_qt	390.57	36.12	0.76
MOL000492	(+)-catechin	290.29	54.83	0.24
MOL005360	malkanguninn	432.56	57.71	0.63
MOL000627	Stepholidine	327.41	33.11	0.54
MOL007213	Nuciferin	295.41	34.43	0.4
MOL000783	Protoporphyrin	562.72	30.86	0.56
MOL000787	Fumarine	353.4	59.26	0.83
MOL008034	21302-79-4	486.76	73.52	0.77
MOL008647	Moupinamide	313.38	86.71	0.26
MOL002773	beta-carotene	536.96	37.18	0.58
MOL000096	(-)-catechin	290.29	49.68	0.24
MOL000098	quercetin	302.25	46.43	0.28
MOL013357	(3S,6R,8S,9S,10R,13R,14S,17R)-17-[(1R,4R)-4-ethyl-1,5-dimethylhexyl]-10,13-dimethyl-2,3,6,7,8,9,11,12,14,15,16,17-dodecahydro-1H-cyclopenta[a]phenanthrene-3,6-diol	430.79	34.37	0.78
Bei Sha Shen (Glehniae Radix)				
MOL001939	Alloisoimperatorin	270.3	34.8	0.22
MOL001941	Ammidin	270.3	34.55	0.22
MOL001942	isoimperatorin	270.3	45.46	0.23
MOL001951	Bergaptin	338.43	41.73	0.42
MOL001956	Cnidilin	300.33	32.69	0.28
MOL000358	beta-sitosterol	414.79	36.91	0.75
MOL000449	Stigmasterol	412.77	43.83	0.76
MOL000098	quercetin	302.25	46.43	0.28
Mai Dong (Ophiopogon Japonicus)				
MOL000358	beta-sitosterol	414.79	36.91	0.75
Tai Zi Shen (Pseudostellariae Radix)				
MOL001506	Supraene	410.8	33.55	0.42
MOL001689	acacetin	284.28	34.97	0.24
MOL001790	Linarin	592.6	39.84	0.71
MOL000358	beta-sitosterol	414.79	36.91	0.75
MOL000006	luteolin	286.25	36.16	0.25
MOL006554	Taraxerol	426.8	38.4	0.77
MOL006756	Schottenol	414.79	37.42	0.75
MOL002464	1-Monolinolein	354.59	37.18	0.3
Wu Wei Zi (Schisandrae Chinensis Fructus)				
MOL004624	Longikaurin A	348.48	47.72	0.53
MOL005317	Deoxyharringtonine	515.66	39.27	0.81
MOL008956	Angeloylgomisin O	498.62	31.97	0.85
MOL008957	Schizandrer B	514.62	30.71	0.83
MOL008968	Gomisin-A	416.51	30.69	0.78
MOL008974	Gomisin G	508.61	32.68	0.83
MOL008978	Gomisin R	400.46	34.84	0.86
MOL008992	Wuweizisu C	384.46	46.27	0.84
Cang Zhu (Atractylodes Lancea)				
MOL000173	wogonin	284.28	30.68	0.23
MOL000179	2-Hydroxyisoxypropyl-3-hydroxy-7-isopentene-2,3-dihydrobenzofuran-5-carboxylic	306.39	45.2	0.2
MOL000184	NSC63551	412.77	39.25	0.76
MOL000186	Stigmasterol 3-O-beta-D-glucopyranoside_qt	412.77	43.83	0.76
MOL000188	3β-acetoxyatractylone	274.39	40.57	0.22
MOL000085	beta-daucosterol_qt	414.79	36.91	0.75
MOL000088	beta-sitosterol 3-O-glucoside_qt	414.79	36.91	0.75
MOL000092	daucosterin_qt	414.79	36.91	0.76
MOL000094	daucosterol_qt	414.79	36.91	0.76
Jie Geng (Platycodon Grandiforus)				
MOL001689	acacetin	284.28	34.97	0.24
MOL004355	Spinasterol	412.77	42.98	0.76
MOL004580	cis-Dihydroquercetin	304.27	66.44	0.27
MOL005996	2-O-methyl-3—O-β-D-glucopyranosyl platycogenate A	739.01	45.15	0.25
MOL000006	luteolin	286.25	36.16	0.25
MOL006026	dimethyl 2-O-methyl-3-O-a-D-glucopyranosyl platycogenate A	739.01	39.21	0.25
MOL006070	robinin	592.6	39.84	0.71
Xing Ren (Amygdalus Communis Vas)				
MOL010921	estrone	270.4	53.56	0.32
MOL010922	Diisooctyl succinate	342.58	31.62	0.23
MOL002211	11,14-eicosadienoic acid	308.56	39.99	0.2
MOL002372	(6Z,10E,14E,18E)-2,6,10,15,19,23-hexamethyltetracosa-2,6,10,14,18,22-hexaene	410.8	33.55	0.42
MOL000359	sitosterol	414.79	36.91	0.75
MOL000449	Stigmasterol	412.77	43.83	0.76
MOL005030	gondoic acid	310.58	30.7	0.2
MOL000953	CLR	386.73	37.87	0.68
MOL000211	Mairin	456.78	55.38	0.78
MOL000492	(+)-catechin	290.29	54.83	0.24
MOL002311	Glycyrol	366.39	90.78	0.67
MOL003410	Ziziphin_qt	472.78	66.95	0.62
MOL004355	Spinasterol	412.77	42.98	0.76
MOL004841	Licochalcone B	286.3	76.76	0.19
MOL004903	liquiritin	418.43	65.69	0.74
MOL004908	Glabridin	324.4	53.25	0.47
MOL005017	Phaseol	336.36	78.77	0.58
MOL007207	Machiline	285.37	79.64	0.24
MOL012922	l-SPD	327.41	87.35	0.54

Table S1: Details of all bioactive ingredient information.

Potential targets of FYQFD against COVID-19 associated lung and kidney injury

The TCMSP databases were searched for candidate targets of active FYQFD ingredients. After fishing for targets, 251 targets were found

for all active FYQFD ingredients after removing duplication. For identification of disease target, 6400 target genes that occur in "Lung Injury" and 6354 in "Kidney Injury" were identified from the GeneCards database. 227 target genes overlapped among FYQFD targts, lung and kidney injury associated targets, were selected as potential targets for further analysis (Figure 1A). The complete list of 227 target genes against COVID-19 associated lung and kidney injury was provided in Supplementary Table S2

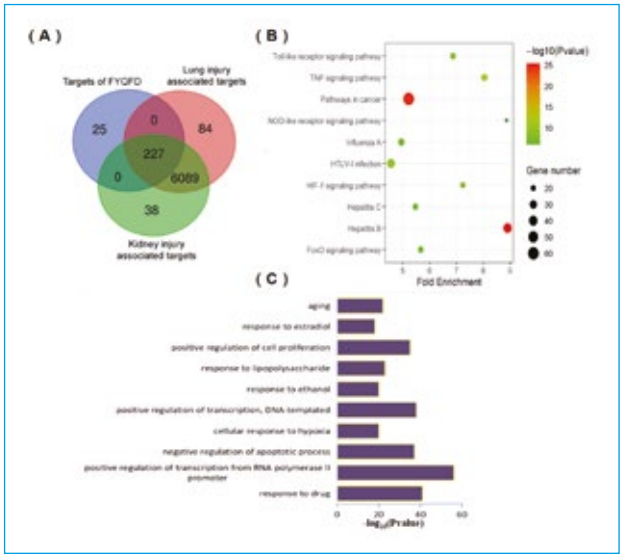

Fig. 1: Identification of drug-disease targets and enrichment analysis. (**A**) The venn diagram of Fangyi Qingfei Decoction (FYQFD) targets, lung and kidney injury associated targets. (**B**) KEGG pathway in the enrichment analysis of target genes associated lung and kidney injury. (**C**) The representative Gene Ontology (GO) biological process (BP) terms in the enrichment analysis of target genes associated lung and kidney injury.

AKT1 ALB IL6 TP53 VEGFA TNF JUN CASP3 EGFR MAPK1 MYC EGF FOS MAPK8 PTGS2 CXCL8 MMP9 ESR1 CCND1 PTEN HSP90AA1 CAT FN1 IL1B ERBB2 NOS3 IL10 CCL2 MMP2 PPARG RELA MAPK14 CTNNB1 BCL2L1 APP CASP8 CDKN2A HMOX1 SERPINE1 ICAM1 STAT1 IL4 CDKN1A CAV1 IL2 HIF1A CASP9 VCAM1 SPP1 MDM2 KDR MCL1 TGFB1 IFNG CRP MPO CXCL10 CDK4 MMP3 NFKBIA F2 PGR MMP1 AHR XIAP CDK2 SOD1 CCNB1 PLAU FASLG PARP1 GSK3B SELE RB1 NFE2L2 IGFBP3 PRKCA IGF2 CXCL2 CCNA2 CD40LG APOB HSPB1 HSPA5 PPARA MET RUNX2 F3 CHEK1 RAF1 SLC2A4 NQO1 CASP7 IL1A GJA1 CYP3A4 IKBKB ESR2 IRF1 NOS1 OPRM1 NCF1 CXCL11 PRKCB CALM1 PTPN1 CHEK2 CYP1A1 PRKCD ADRB2 BIRC5 COL1A1 PRKACA E2F1 DRD2 CYP19A1 CTSD TOP2A BCL2 ERBB3 ALOX5 SLC2A1 GSTP1 BAX CHUK NCOA1 DRD4 PLAT NCOA2 TOP1 CYP2B6 ADRA2A DPP4 RXRA SLC6A3 MAOA HTR3A THBD PPP3CA MMP10 ADRA2C CHRM2 CYP1B1 OPRK1 PTGER3 FASN GSTM1 OPRD1 MAOB ADRA2B PCNA INSR CYP1A2 DRD3 HTR2C PTGS1 NR1I2 HTR2A PON1 OLR1 SLC6A2 E2F2 RASA1 ADRA1B CHRM1 GRIA2 GSTM2 MGAM PTGES HSF1 ACACA ADRA1A ADRA1D HK2 BBC3 PIK3CG ADRB1 ODC1 POR DRD1 TYR CD14 PPARD GABRA2 DRD5 SLPI NR1I3 GABRA1 DUOX2 RXRB NR3C2 F7 KCNH2 XDH HAS2 F10 LBP CHRM3 KCNMA1 SCN5A CHRNA7 CACNA1S MTTP PIM1 LTA4H ELK1 GABRA6 AKR1C1 PRSS1 NKX3-1 PDE4D AKR1B10 ADH1C DGAT2 CLDN4 GABRA3 CHRNA2 PYGM NPEPPS CA2 RUNX1T1 PDE3A EIF6 ACPP COL8A1 ABCA2 CLOO

Table S2: The complete list of 227 target genes associated lung and kidney injury (ordered by degree in PPI network).

KEGG and GO pathway analysis

To explore the potential mechanism related to these candidate targets, KEGG pathway analysis was performed. Based on filter conditions of $p < 0.05$, KEGG pathway analysis returned 137 items, including pathways in cancer, Hepatitis B, Hepatitis C, Pancreatic cancer, TNF signaling pathway, HTLV-I infection, PI3K-Akt signaling pathway, Toll-like receptor signaling pathway, NOD-like receptor signaling pathway, Influenza A, FoxO signaling pathway and so on (Figure 1B, supplementary Table S3). Bio-functions of this module primarily involved oxidation-reduction process, fatty acid beta-oxidation, metabolic process and fatty acid beta-oxidation using acyl-CoA dehydrogenase, and so on. Bio-functions of those genes primarily involved response to drug, cellular response to hypoxia, response to ethanol, response to estradioland so on (Figure 1C, supplementary Table S4). These items revealed that the potential pathways affected by FYQFD mainly involved aspects of improving immunity, anti-inflammatory effects, fighting against viruses and other pathogens.

KEGG NO.	Pathway Term	Count	%	FDR
hsa05200	Pathways in cancer	62	0.18	2.21E-25
hsa05161	Hepatitis B	39	0.12	4.85E-23
hsa05219	Bladder cancer	20	0.06	9.13E-16
hsa05215	Prostate cancer	26	0.08	2.96E-15
hsa05212	Pancreatic cancer	23	0.07	5.21E-15
hsa04668	TNF signaling pathway	26	0.08	4.22E-13
hsa05222	Small cell lung cancer	23	0.07	3.41E-12
hsa05205	Proteoglycans in cancer	33	0.1	3.83E-12
hsa05223	Non-small cell lung cancer	19	0.06	1.94E-11
hsa05166	HTLV-I infection	35	0.1	1.11E-10
hsa05220	Chronic myeloid leukemia	20	0.06	2.00E-10
hsa05142	Chagas disease (American trypanosomiasis)	23	0.07	3.13E-10
hsa05214	Glioma	19	0.06	3.58E-10
hsa04151	PI3K-Akt signaling pathway	39	0.12	1.76E-09
hsa05210	Colorectal cancer	18	0.05	2.02E-09
hsa04620	Toll-like receptor signaling pathway	22	0.07	4.37E-09
hsa04066	HIF-1 signaling pathway	21	0.06	5.49E-09
hsa04115	p53 signaling pathway	18	0.05	8.07E-09
hsa04919	Thyroid hormone signaling pathway	22	0.07	2.28E-08
hsa04210	Apoptosis	17	0.05	2.61E-08
hsa05164	Influenza A	26	0.08	6.04E-08
hsa04068	FoxO signaling pathway	23	0.07	6.60E-08
hsa05145	Toxoplasmosis	21	0.06	7.70E-08
hsa04660	T cell receptor signaling pathway	20	0.06	1.07E-07
hsa05140	Leishmaniasis	17	0.05	2.41E-07
hsa05218	Melanoma	17	0.05	2.41E-07
hsa05213	Endometrial cancer	15	0.04	2.65E-07
hsa05160	Hepatitis C	22	0.07	3.96E-07
hsa05133	Pertussis	17	0.05	5.78E-07
hsa04020	Calcium signaling pathway	25	0.07	6.57E-07
hsa04621	NOD-like receptor signaling pathway	15	0.04	7.83E-07
hsa04080	Neuroactive ligand-receptor interaction	31	0.09	8.23E-07
hsa04010	MAPK signaling pathway	29	0.09	1.98E-06
hsa05152	Tuberculosis	24	0.07	2.90E-06
hsa04064	NF-kappa B signaling pathway	17	0.05	5.82E-06
hsa04510	Focal adhesion	25	0.07	1.17E-05
hsa04380	Osteoclast differentiation	20	0.06	1.25E-05
hsa05144	Malaria	13	0.04	1.78E-05
hsa04931	Insulin resistance	18	0.05	2.22E-05
hsa05014	Amyotrophic lateral sclerosis (ALS)	13	0.04	2.27E-05
hsa04932	Non-alcoholic fatty liver disease (NAFLD)	21	0.06	2.47E-05
hsa04024	cAMP signaling pathway	24	0.07	2.58E-05
hsa04370	VEGF signaling pathway	14	0.04	2.67E-05
hsa05143	African trypanosomiasis	11	0.03	3.17E-05
hsa04915	Estrogen signaling pathway	17	0.05	4.04E-05
hsa04012	ErbB signaling pathway	16	0.05	4.50E-05
hsa04728	Dopaminergic synapse	19	0.06	5.12E-05
hsa05134	Legionellosis	13	0.04	5.78E-05
hsa05162	Measles	19	0.06	9.39E-05
hsa05146	Amoebiasis	17	0.05	1.09E-04
hsa05202	Transcriptional misregulation in cancer	21	0.06	1.38E-04
hsa05169	Epstein-Barr virus infection	18	0.05	1.42E-04
hsa04917	Prolactin signaling pathway	14	0.04	1.81E-04
hsa04110	Cell cycle	18	0.05	1.82E-04
hsa05230	Central carbon metabolism in cancer	13	0.04	4.25E-04
hsa05206	MicroRNAs in cancer	27	0.08	4.58E-04
hsa04071	Sphingolipid signaling pathway	17	0.05	6.34E-04
hsa04722	Neurotrophin signaling pathway	17	0.05	6.34E-04

hsa05221	Acute myeloid leukemia	12	0.04	8.15E-04
hsa05132	Salmonella infection	14	0.04	1.20E-03
hsa04726	Serotonergic synapse	16	0.05	1.23E-03
hsa04022	cGMP-PKG signaling pathway	19	0.06	1.31E-03
hsa05323	Rheumatoid arthritis	14	0.04	2.39E-03
hsa05321	Inflammatory bowel disease (IBD)	12	0.04	3.29E-03
hsa04912	GnRH signaling pathway	14	0.04	3.52E-03
hsa04910	Insulin signaling pathway	17	0.05	4.23E-03
hsa05031	Amphetamine addiction	12	0.04	4.51E-03
hsa04014	Ras signaling pathway	22	0.07	4.67E-03
hsa05020	Prion diseases	9	0.03	6.94E-03
hsa04662	B cell receptor signaling pathway	12	0.04	7.08E-03
hsa04920	Adipocytokine signaling pathway	12	0.04	8.18E-03
hsa04540	Gap junction	13	0.04	1.41E-02
hsa05216	Thyroid cancer	8	0.02	2.29E-02
hsa05120	Epithelial cell signaling in Helicobacter pylori infection	11	0.03	3.47E-02
hsa05168	Herpes simplex infection	18	0.05	4.12E-02

Table S3: KEGG pathway term of target genes associated associated lung and kidney injury significantly enriched (FDR < 0.05).

GO No.	biological process (BP) Term	Count	%	FDR
GO:0042493	response to drug	41	0.12	5.10E-25
GO:0045944	positive regulation of transcription from RNA polymerase II promoter	56	0.17	4.95E-17
GO:0043066	negative regulation of apoptotic process	37	0.11	9.30E-15
GO:0071456	cellular response to hypoxia	20	0.06	4.65E-14
GO:0045893	positive regulation of transcription, DNA-templated	38	0.11	7.19E-14
GO:0045471	response to ethanol	20	0.06	2.00E-13
GO:0032496	response to lipopolysaccharide	23	0.07	7.99E-13
GO:0008284	positive regulation of cell proliferation	35	0.10	1.19E-12
GO:0032355	response to estradiol	18	0.05	6.76E-12
GO:0007568	aging	22	0.07	1.15E-11
GO:0071222	cellular response to lipopolysaccharide	19	0.06	1.93E-11
GO:0001666	response to hypoxia	22	0.07	2.66E-11
GO:0010628	positive regulation of gene expression	25	0.07	2.14E-10
GO:0097192	extrinsic apoptotic signaling pathway in absence of ligand	12	0.04	7.65E-10
GO:0006915	apoptotic process	33	0.10	9.82E-09
GO:0009636	response to toxic substance	15	0.04	1.18E-08
GO:0045907	positive regulation of vasoconstriction	11	0.03	1.36E-08
GO:0033663	lipopolysaccharide-mediated signaling pathway	11	0.03	1.36E-08
GO:0045429	positive regulation of nitric oxide biosynthetic process	12	0.04	1.38E-08
GO:0006954	inflammatory response	27	0.08	1.56E-08
GO:0045766	positive regulation of angiogenesis	16	0.05	6.63E-08
GO:0071880	adenylate cyclase-activating adrenergic receptor signaling pathway	9	0.03	1.09E-07
GO:0001525	angiogenesis	20	0.06	3.02E-07
GO:0046677	response to antibiotic	10	0.03	4.56E-07
GO:0071407	cellular response to organic cyclic compound	12	0.04	5.58E-07
GO:0008285	negative regulation of cell proliferation	25	0.07	1.31E-06
GO:0001934	positive regulation of protein phosphorylation	15	0.04	2.92E-06
GO:0048146	positive regulation of fibroblast proliferation	11	0.03	3.91E-06
GO:0071356	cellular response to tumor necrosis factor	14	0.04	4.79E-06
GO:0007165	signal transduction	43	0.13	5.23E-06
GO:0030168	platelet activation	14	0.04	8.32E-06
GO:0001975	response to amphetamine	9	0.03	9.94E-06
GO:0051591	response to cAMP	10	0.03	1.52E-05

GO:0070374	positive regulation of ERK1 and ERK2 cascade	16	0.05	2.48E-05
GO:0043065	positive regulation of apoptotic process	20	0.06	4.19E-05
GO:0030335	positive regulation of cell migration	16	0.05	4.89E-05
GO:0071260	cellular response to mechanical stimulus	11	0.03	6.18E-05
GO:0032930	positive regulation of superoxide anion generation	6	0.02	8.92E-05
GO:0043401	steroid hormone mediated signaling pathway	10	0.03	1.09E-04
GO:0097421	liver regeneration	8	0.02	1.54E-04
GO:0006805	xenobiotic metabolic process	11	0.03	1.55E-04
GO:0043525	positive regulation of neuron apoptotic process	9	0.03	1.59E-04
GO:0042060	wound healing	11	0.03	1.99E-04
GO:0043536	positive regulation of blood vessel endothelial cell migration	7	0.02	2.27E-04
GO:0010332	response to gamma radiation	8	0.02	2.53E-04
GO:0006919	activation of cysteine-type endopeptidase activity involved in apoptotic process	11	0.03	2.83E-04
GO:0051091	positive regulation of sequence-specific DNA binding transcription factor activity	12	0.04	2.89E-04
GO:0042220	response to cocaine	8	0.02	3.20E-04
GO:0008630	intrinsic apoptotic signaling pathway in response to DNA damage	9	0.03	3.29E-04
GO:0043627	response to estrogen	10	0.03	3.54E-04
GO:0009408	response to heat	9	0.03	3.91E-04
GO:0007200	phospholipase C-activating G-protein coupled receptor signaling pathway	10	0.03	4.05E-04
GO:0006468	protein phosphorylation	23	0.07	4.05E-04
GO:0010629	negative regulation of gene expression	13	0.04	5.70E-04
GO:0035690	cellular response to drug	10	0.03	5.99E-04
GO:0033138	positive regulation of peptidyl-serine phosphorylation	10	0.03	6.80E-04
GO:0009409	response to cold	8	0.02	7.59E-04
GO:0006874	cellular calcium ion homeostasis	11	0.03	8.37E-04
GO:0035094	response to nicotine	8	0.02	9.25E-04
GO:0008283	cell proliferation	20	0.06	9.34E-04
GO:0018107	peptidyl-threonine phosphorylation	8	0.02	1.12E-03
GO:0048148	behavioral response to cocaine	6	0.02	1.34E-03
GO:0018105	peptidyl-serine phosphorylation	12	0.04	1.70E-03
GO:0051592	response to calcium ion	9	0.03	1.77E-03
GO:0050999	regulation of nitric-oxide synthase activity	7	0.02	1.78E-03
GO:0043406	positive regulation of MAP kinase activity	9	0.03	2.02E-03
GO:0007566	embryo implantation	8	0.02	2.29E-03
GO:0007595	lactation	8	0.02	2.29E-03
GO:0048661	positive regulation of smooth muscle cell proliferation	9	0.03	2.31E-03
GO:0055114	oxidation-reduction process	25	0.07	2.58E-03
GO:0006940	regulation of smooth muscle contraction	6	0.02	2.86E-03
GO:0035994	response to muscle stretch	6	0.02	2.86E-03
GO:0006977	DNA damage response, signal transduction by p53 class mediator resulting in cell cycle arrest	9	0.03	2.98E-03
GO:0051092	positive regulation of NF-kappaB transcription factor activity	12	0.04	3.16E-03
GO:0007267	cell-cell signaling	16	0.05	3.17E-03
GO:0051897	positive regulation of protein kinase B signaling	10	0.03	3.27E-03
GO:0071363	cellular response to growth factor stimulus	8	0.02	3.72E-03
GO:0043200	response to amino acid	7	0.02	5.39E-03
GO:0050665	hydrogen peroxide biosynthetic process	5	0.01	6.72E-03
GO:0008637	apoptotic mitochondrial changes	6	0.02	7.38E-03
GO:0007265	Ras protein signal transduction	9	0.03	7.59E-03
GO:0043491	protein kinase B signaling	7	0.02	7.93E-03
GO:0051402	neuron apoptotic process	7	0.02	7.93E-03
GO:1902042	negative regulation of extrinsic apoptotic signaling pathway via death domain receptors	7	0.02	7.93E-03
GO:2001244	positive regulation of intrinsic apoptotic signaling pathway	7	0.02	7.93E-03
GO:0071347	cellular response to interleukin-1	9	0.03	8.46E-03
GO:0097190	apoptotic signaling pathway	9	0.03	8.46E-03
GO:0006974	cellular response to DNA damage stimulus	14	0.04	8.51E-03
GO:0042542	response to hydrogen peroxide	8	0.02	8.87E-03
GO:0034097	response to cytokine	8	0.02	1.01E-02
GO:0050900	leukocyte migration	11	0.03	1.02E-02
GO:0045080	positive regulation of chemokine biosynthetic process	5	0.01	1.11E-02
GO:0006367	transcription initiation from RNA polymerase II promoter	12	0.04	1.16E-02
GO:0007623	circadian rhythm	9	0.03	1.28E-02
GO:0032869	cellular response to insulin stimulus	9	0.03	1.56E-02
GO:2001240	negative regulation of extrinsic apoptotic signaling pathway in absence of ligand	7	0.02	1.59E-02
GO:0007271	synaptic transmission, cholinergic	7	0.02	1.59E-02
GO:0001994	norepinephrine-epinephrine vasoconstriction involved in regulation of systemic arterial blood pressure	4	0.01	1.68E-02
GO:0002576	platelet degranulation	10	0.03	1.79E-02
GO:0070301	cellular response to hydrogen peroxide	8	0.02	1.89E-02
GO:0035924	cellular response to vascular endothelial growth factor stimulus	6	0.02	2.04E-02
GO:0007194	negative regulation of adenylate cyclase activity	6	0.02	2.04E-02
GO:0032570	response to progesterone	7	0.02	2.18E-02
GO:0000165	MAPK cascade	15	0.04	2.22E-02
GO:0043410	positive regulation of MAPK cascade	9	0.03	2.28E-02
GO:0045892	negative regulation of transcription, DNA-templated	21	0.06	2.39E-02
GO:0000187	activation of MAPK activity	10	0.03	2.44E-02
GO:0007190	activation of adenylate cyclase activity	7	0.02	2.54E-02
GO:0042738	exogenous drug catabolic process	5	0.01	2.56E-02
GO:0090399	replicative senescence	5	0.01	2.56E-02
GO:0006955	immune response	19	0.06	2.78E-02
GO:0007626	locomotory behavior	9	0.03	2.98E-02
GO:0009615	response to virus	10	0.03	3.05E-02
GO:0051090	regulation of sequence-specific DNA binding transcription factor activity	6	0.02	3.16E-02
GO:0001541	ovarian follicle development	7	0.02	3.40E-02
GO:0001963	synaptic transmission, dopaminergic	5	0.01	3.65E-02
GO:0006809	nitric oxide biosynthetic process	5	0.01	3.65E-02
GO:0051926	negative regulation of calcium ion transport	5	0.01	3.65E-02
GO:0060134	prepulse inhibition	5	0.01	3.65E-02
GO:0045840	positive regulation of mitotic nuclear division	6	0.02	3.87E-02
GO:0030574	collagen catabolic process	8	0.02	4.11E-02
GO:0031622	positive regulation of fever generation	4	0.01	4.17E-02
GO:0010575	positive regulation of vascular endothelial growth factor production	6	0.02	4.69E-02

Table S4: Gene ontology(GO) biological process(BP) term of target genes associated associated lung and kidney injury significantly enriched (FDR < 0.05).

Construction of herbs - ingredient - targets network and analysis

The STRING database was used to explored PPI relationships of potential protein targets of FYQFD as related to the treatment of COVID-19. By using these targets, the network of PPI relationships was shown to contain 226 nodes (excluding CLOQ, which no interaction with other proteins) and 4511 edges (representing the interaction between the active proteins and proteins), with a median node degree of 30.5. Next, the top 10 targets ranked by the degree method were identified as hub genes by use of the cytoHubba plug-in. These targets included

AKT1, ALB, IL6, TP53, VEGFA, TNF, JUN, CASP3, EGFR and MAPK1. After preliminary construction, the drug compound target network was screened and subtracted according to the median degree value. Finally, the network consisted of 169 nodes and 3510 edges, including 14 TCM nodes, 43 component nodes and 112 targets (Figure 2). The top 10 compounds ranked by degree were mol000098 (quercetin), mol000422 (kaempferol), mol000006 (luteolin), mol000173 (wogonin), mol000378 (7-o-methylosmuronalatol), mol000354 (isorhamnetin), mol000449 (stigmasterol), mol012922 (l-spd), mol000627 (stephalidine), mol001689 (acacetin).

Fig. 2: Construction of herbs - ingredient - targets network of Fangyi Qingfei Decoction (FYQFD). Only target genes with degree more than 30 were exhibited.

Molecular docking

In order to further identify the relationship between hub components and genes, the top ten core targets and core components were extracted from the network. The results showed that nine of the core targets (except ALB) were mainly regulated by five components from Bai Shao, Huang Qi, Bei Sha Shen, Da Zao, Fang Feng, Cang Zhu, Jie Geng, Tai Zi Shen and Xing Ren (Figure. 5), which were MOL000422 (kaempferol), MOL000098 (quercetin), MOL000173 (wogonin), MOL000006 (luteolin), MOL001689 (acacetin), respectively. The results of molecular docking showed that the binding energies of the five active compounds with each target ranged from - 14.19 to - 34.24 kJ / mol (Figure. 3), indicating that the core targets and the active components had a good binding and thus were selected to further study.

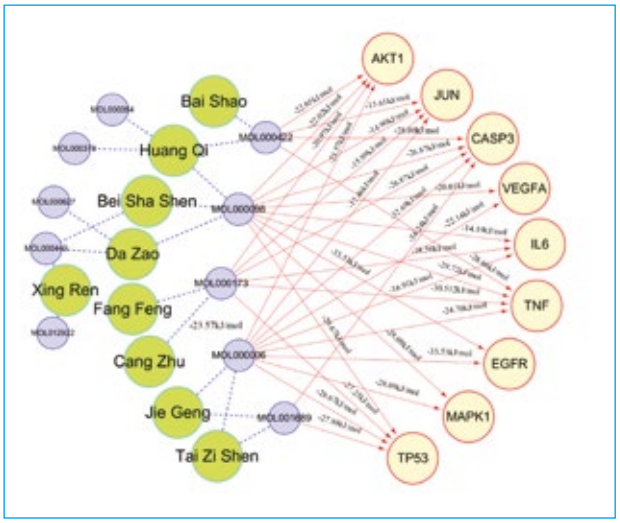

Fig. 3: Molecular docking of hub compounds with hub targets.

Docking results of active components with ACE2 protein and SARS-CoV-2 3CLpro

With the tracing of COVID-19 and the discovery of its gene sequence, and the analysis of the structure of the spike protein of new coronavirus by freeze electron microscopy, SARS-CoV-2 3CLpro and ACE2 have become popular targets for screening anti COVID-19. In this study, based on the above analysis, we used these five active compounds to mimic molecular docking with SARS-CoV-2 3CLpro and ACE2, and compared with the currently recommended clinical use of remdesivir. Affinity was evaluated from the molecular docking, and when the affinity score was lower, the binding affinity was stronger.

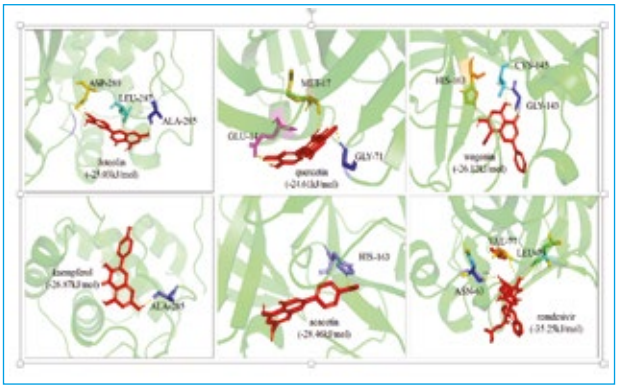

Fig. 4: Molecular docking of SARS-CoV-2 3CL hydrolase with kaempferol, quercetin, wogonin, luteolin, acacetin and remdesivir.

The results showed that luteolin (binding energy -25.03kJ/mol), quercetin (binding energy -24.61 kJ/mol), wogonin (binding energy -26.12kJ/mol), kaempferol (binding energy -28.87 kJ/mol), acacetin (binding energy -28.46 kJ/mol) can bind to

SARS-CoV-2 3CLpro through hydrogen bonds (Figure 4), however, the binding ability is slightly lower than that of remdesivir (binding energy -35.25kj/mol). On the other hand, luteolin (binding energy -27.59 kJ/mol), quercetin (binding energy -25.53kJ/mol), wogonin (binding energy -30.01kJ/mol), kaempferol (binding energy -27.38kJ/mol) and robinin (binding energy -26.33 kJ/mol) showed higher binding capacity to ACE2, compared to remdesivir (binding energy -24.57kJ/mol) (Figure 5).

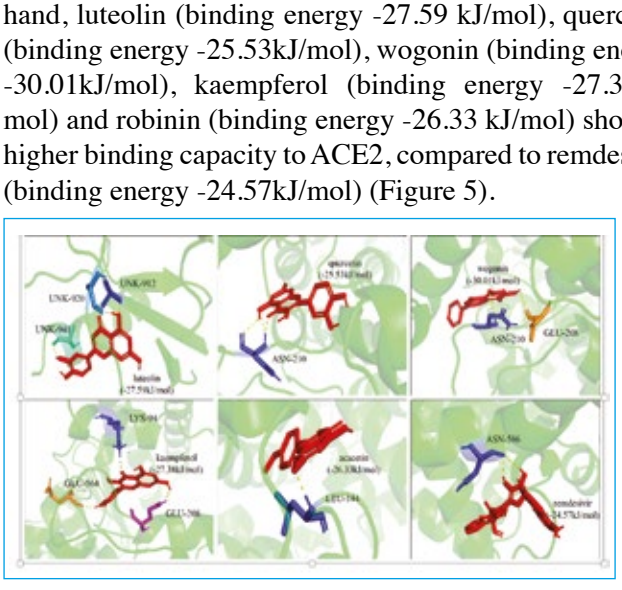

Fig. 5: Molecular docking of ACE2 with kaempferol, quercetin, wogonin, luteolin, acacetin and remdesivir.

Discussion

SARS-CoV-2 infection can lead to multiple organ failure such as lung, myocardium, kidney and so on. This infection developed in rapidly some patients and even caused the death of multiple organ failure (MOF). With the observation of renal pathology, the AKI (acute renal injury) caused by COVID-19 has attracted more and more attention. Clinical evidence also shows that the ICU patients of COVID-19 had a higher incidence rates of AKI compared to non-ICU patients. Meanwhile, It has been reported that the Scr (serum creatinine), BUN (blood urea nitrogen), proteinuria and hematuria were the independent influencing factors of mortality in patients with COVID-19[15]. Therefore, the best treatment strategy for covid-19 should not only improve the respiratory system function of patients, but also delay the decline of renal function.

In present study, we performed the network pharmacology technology and as a consequence, a total of 227 potential targets related to human acute lung and kidney injury of FYQFD were identified by means of active component screening, target prediction and network analysis. By constructing the target protein interaction network and calculating the degree, the top ten targets were detected as follows: AKT1, ALB, IL6, TP53, VEGFA, TNF, Jun, CASP3, EGFR, MAPK1. The bio-function enrichment analysis of all the targets showed that these targets potentially involved the regulation of cancer pathway, hepatitis B, influenza virus, TNF signaling pathway, PI3K-Akt pathway, toll-like pathway and so on. According to previous studies, these core genes and enrichment pathways have been reported to participate in the progress of various viral or infectious diseases. In particular, it is apparent that SARS-CoV-2 infection has two clear clinical phases of infection: the former which involves the viral infection and replication[16], and the inflammatory phase which often leads to rapid deterioration and worsening respiratory symptoms, requiring hospital admission to avoid deterioration[17]. Therefore, there is a proposal that the in silico screening of hyper-inflammative chemicals for targeted immunomodulation is beneficial for the development of new drugs to improve mortality. For example, recent studies found that sars-cov-2 induced lymphocyte apoptosis and activation of TP53 signaling pathway may be the cause of lymphopenia[18].

On the other hand, many further studies shown that inhibitors of these pathways or core targets often contribute to the remission of viral diseases or inflammation. For example, inhibitor of PI3K-Akt pathway can help to improve the pneumonia caused by viral HIN1 and improve the prognosis[19]. Therefore, some scholars recently proposed that PI3K-Akt inhibitors may be potential targets for covid-19 treatment[20]. At the same time, some scholars used lipopolysaccharide (LPS) to establish a rat lung injury model to simulate the pathological symptoms of covid-19, the results showed that Qingfei Paidu decoction could delay inflammatory factor storm by inhibiting toll like pathway and alleviate the disease[21]. Taken together, the active ingredients of FYQFD can improve COVID-19-related lung and kidney injury through these signaling pathways and antiviral effects theoretically.

Accumulating evidences supported that TCM is a great deal of experience in the prevention and treatment of epidemics in the past. In our work, by constructing a sub-network of 10 core compounds and 10 target proteins, we found that 9 of the 10 target proteins (except ALB) were mainly regulated by five active compounds from eight herbs, they were mol000422 (kaempferol), mol000098 (quercetin), mol000173 (wogonin), mol000006 (luteolin) and mol001689 (Robinia pseudoacacia), respectively. Among them, quercetin from Astragalus membranaceus, Radix Glehniae and Zizyphus jujuba has the potential to regulate nine target proteins. Previous studies have shown that quercetin demonstrated an antiviral efficacy in hepatitis C patients[22] and influenza A virus (IAV) H1N1 infection[23] with high safety. While kaempferol from Radix Paeoniae Alba and Astragalus membranaceus has many biological functions, such as anti-inflammatory, anti-

oxidation, anti-virus, enhancing immune function[24]. Further, kaempferol can inhibit the expression of TNF - α, IL-6 and other inflammatory factors by eliminating oxygen free radicals or reducing the activities of MAPK[25] and PI3K / Akt[26] signal pathway. After preliminary screening, the binding affinity between the 5 hub constituents and the 9 hub genes was calculated, the molecular docking results showed that the binding energies ranged from - 14.19 to - 34.24 kJ/mol, which indicated that the 5 hub constituents can bind to potential targets well, according to the screening criteria of the binding energy ≤ -5.0 kj/mol[27].

With tracing SARS-CoV-2, exporing its gene sequence, and analysing the freeze electron microscope structure of the spike protein of new coronavirus, SARS-CoV-2 3CLpro[28] and ACE2[29] have became popular targets for screening anti SARS-CoV-2 drugs. The SARS-CoV-2 3CLpro (PDB: 6LU7) is required for the replication of coronaviruses and considered a validated target in the design of potential anti-coronavirus inhibitors[30]. While both SARS-CoV-2 and SARS-CoV enter host cells via the ACE2 receptor, which is expressed in various human organs[31].Thus both of these two proteins have been considered as validated targets in the design of potential anti-coronavirus inhibitors. In present study, a computational strategy for modeling molecular docking was used to evaluate the affinity between candidate constituents and SARS-CoV-2 3CLpro and ACE2, this technique helps to identify FYQFD constituents that may interact directly with SARS-CoV-2 or ACE2. These results indicate that the bioactive constituents of FYQFD might possess direct anti-SARS-CoV-2 activity in addition to their effects on the body.

In short, in an attempt to provide a possible therapeutic schedule for COVID-19, a network pharmacology method and molecular docking technology were integrated to predict the mechanism through which FYQFD improves COVID-19. The results demonstrated a synergistic effect among herbs and illustrated that FYQFD could play pharmacological roles in the treatment of COVID-19 through multi-component or multi-targeted pathway effects at the molecular level, mainly involving anti-viral, immune-regulatory, and anti-inflammatory actions. These findings may offer a reference basis for further investigations of the mechanism by which FYQFD exerts effects against COVID-19. Nevertheless, further experiments are needed to support our findings.

References

1) Singhal T. A Review of Coronavirus Disease-2019 (COVID-19). Indian J Pediatr. 2020; 87(4): 281-286.
2) Song P, Karako T. COVID-19: Real-time dissemination of scientific information to fight a public health emergency of international concern. Biosci Trends. 2020; 14(1): 1-2.
3) Watchorn J, Huang DY, Joslin J, Bramham K, Hutchings SD. Critically ILL COVID-19 Patients With Acute Kidney Injury Have Reduced Renal Blood Flow and Perfusion Despite Preserved Cardiac Function; A Case-Control Study Using Contrast Enhanced Ultrasound. Shock. 2020.
4) Werion A, Belkhir L, Perrot M, et al. SARS-CoV-2 Causes a Specific Dysfunction of the Kidney Proximal Tubule. Kidney Int. 2020.
5) Li Z, Wu M, Yao J, et al. Caution on Kidney Dysfunctions of COVID-19 Patients. medRxiv. 2020:2020.2002.2008.20021212.
6) Naicker S, Yang CW, Hwang SJ, Liu BC, Chen JH, Jha V. The Novel Coronavirus 2019 epidemic and kidneys. Kidney Int. 2020; 97(5): 824-828.
7) Tay MZ, Poh CM, Renia L, MacAry PA, Ng LFP. The trinity of COVID-19: immunity, inflammation and intervention. Nat Rev Immunol. 2020; 20(6): 363-374.
8) Puelles VG, Lutgehetmann M, Lindenmeyer MT, et al. Multiorgan and Renal Tropism of SARS-CoV-2. N Engl J Med. 2020; 383(6): 590-592.
9) Du HZ, Hou XY, Miao YH, Huang BS, Liu DH. Traditional Chinese Medicine: an effective treatment for 2019 novel coronavirus pneumonia (NCP). Chin J Nat Med. 2020; 18(3): 206-210.
10) Xue R, Fang Z, Zhang M, Yi Z, Wen C, Shi T. TCMID: Traditional Chinese Medicine integrative database for herb molecular mechanism analysis. Nucleic Acids Res. 2013;41(Database issue): D1089-1095.
11) Ru J, Li P, Wang J, et al. TCMSP: a database of systems pharmacology for drug discovery from herbal medicines. J Cheminform. 2014; 6: 13.
12) Rebhan M, Chalifa-Caspi V, Prilusky J, Lancet D. GeneCards: integrating information about genes, proteins and diseases. Trends Genet. 1997; 13(4): 163.
13) Zhou F, He K, Guan Y, et al. Network pharmacology-based strategy to investigate pharmacological mechanisms of Tinospora sinensis for treatment of Alzheimer's disease. J Ethnopharmacol. 2020; 259: 112940.
14) Hsu CH, Lu CM, Chang TT. Efficacy and safety of modified Mai-Men-Dong-Tang for treatment of allergic asthma. Pediatr Allergy Immunol. 2005; 16(1): 76-81.
15) Diao B, Wang C, Wang R, et al. Human Kidney is a Target for Novel Severe Acute Respiratory Syndrome Coronavirus 2 (SARS-CoV-2) Infection. medRxiv. 2020:2020.2003.2004.20031120.
16) Ruan Q, Yang K, Wang W, Jiang L, Song J. Clinical predictors of mortality due to COVID-19 based on an analysis of data of 150 patients from Wuhan, China. Intensive Care Med. 2020; 46(5): 846-848.
17) Mehta P, McAuley DF, Brown M, et al. COVID-19: consider cytokine storm syndromes and immunosuppression. Lancet. 2020; 395(10229): 1033-1034.

18) Xiong Y, Liu Y, Cao L, et al. Transcriptomic characteristics of bronchoalveolar lavage fluid and peripheral blood mononuclear cells in COVID-19 patients. Emerg Microbes Infect. 2020; 9(1): 761-770.
19) Wang CH, Chung FT, Lin SM, et al. Adjuvant treatment with a mammalian target of rapamycin inhibitor, sirolimus, and steroids improves outcomes in patients with severe H1N1 pneumonia and acute respiratory failure. Crit Care Med. 2014; 42(2): 313-321.
20) Lehrer S. Inhaled biguanides and mTOR inhibition for influenza and coronavirus (Review). World Acad Sci J. 2020; 2(3).
21) Yang R, Liu H, Bai C, et al. Chemical composition and pharmacological mechanism of Qingfei Paidu Decoction and Ma Xing Shi Gan Decoction against Coronavirus Disease 2019 (COVID-19): in silico and experimental study. Pharmacol Res. 2020: 104820.
22) Lu NT, Crespi CM, Liu NM, et al. A Phase I Dose Escalation Study Demonstrates Quercetin Safety and Explores Potential for Bioflavonoid Antivirals in Patients with Chronic Hepatitis C. Phytother Res. 2016; 30(1): 160-168.
23) Vaidya B, Cho SY, Oh KS, et al. Effectiveness of Periodic Treatment of Quercetin against Influenza A Virus H1N1 through Modulation of Protein Expression. J Agric Food Chem. 2016; 64(21): 4416-4425.
24) Imran M, Rauf A, Shah ZA, et al. Chemo-preventive and therapeutic effect of the dietary flavonoid kaempferol: A comprehensive review. Phytother Res. 2019; 33(2): 263-275.
25) Feng H, Cao J, Zhang G, Wang Y. Kaempferol Attenuates Cardiac Hypertrophy via Regulation of ASK1/MAPK Signaling Pathway and Oxidative Stress. Planta Med. 2017; 83(10): 837-845.
26) Kim GD. Kaempferol Inhibits Angiogenesis by Suppressing HIF-1alpha and VEGFR2 Activation via ERK/p38 MAPK and PI3K/Akt/mTOR Signaling Pathways in Endothelial Cells. Prev Nutr Food Sci. 2017; 22(4): 320-326.
27) Zhang ZJ, Wu WY, Hou JJ, et al. Active constituents and mechanisms of Respiratory Detox Shot, a traditional Chinese medicine prescription, for COVID-19 control and prevention: Network-molecular docking-LC-MS(E) analysis. J Integr Med. 2020; 18(3): 229-241.
28) Chen YW, Yiu CB, Wong KY. Prediction of the SARS-CoV-2 (2019-nCoV) 3C-like protease (3CL (pro)) structure: virtual screening reveals velpatasvir, ledipasvir, and other drug repurposing candidates. F1000Res. 2020; 9: 129.
29) Lu R, Zhao X, Li J, et al. Genomic characterisation and epidemiology of 2019 novel coronavirus: implications for virus origins and receptor binding. Lancet. 2020; 395(10224): 565-574.
30) Wu C, Liu Y, Yang Y, et al. Analysis of therapeutic targets for SARS-CoV-2 and discovery of potential drugs by computational methods. Acta Pharm Sin B. 2020; 10(5): 766-788.
31) Ni W, Yang X, Yang D, et al. Role of angiotensin-converting enzyme 2 (ACE2) in COVID-19. Crit Care. 2020; 24(1): 422.

Acknowledgements
We would like to acknowledge the KEGG database developed by Kanehisa Laboratories. We would like to acknowledge the TCMSP and String databases for free use.

Funding
This work was supported by the Medical Scientific Research Project of Health and Family Planning Commission of Jiangsu Province (Z2018026 to WANPENG WANG), and the natural science research project of Huai'an city (Grant No. HAB202011)

Author Contributions
ZHI ZUO, WANPENG WANG conceived and designed the research methods. HUAILIAN LIU, RAN YU, and HAIQING CHEN collected the data; HUAILIAN LIU and KAI LIAO analysed the data and molecular docking; KAI LIAO, and HUAILIAN LIU wrote the original draft. WANPENG WANG reviewed and edited the manuscript. All authors read and approved the final manuscript

Corresponding Author:
Wanpeng Wang
Email: wangwanpeng123@163.com
(China)